

Frustrated Quantum Spin Models with Cold Coulomb Crystals

A. Bermudez,¹ J. Almeida,¹ F. Schmidt-Kaler,² A. Retzker,¹ and M. B. Plenio¹

¹*Institut für Theoretische Physik, Albert-Einstein Allee 11, Universität Ulm, 89069 Ulm, Germany*

²*Institut für Physik, Staudingerweg 7, Johannes Gutenberg-Universität Mainz, 55099 Mainz, Germany*

We exploit the geometry of a zig-zag cold-ion crystal in a linear trap to propose the quantum simulation of a paradigmatic model of long-ranged magnetic frustration. Such a quantum simulation would clarify the complex features of a rich phase diagram that presents ferromagnetic, dimerized antiferromagnetic, paramagnetic, and floating phases, together with previously unnoticed features that are hard to assess by numerics. We analyze in detail its experimental feasibility, and provide supporting numerical evidence on the basis of realistic parameters in current ion-trap technology.

Our understanding of interacting quantum many-body systems is usually hindered by their inherent complexity. In order to unveil their properties, an original approach are the so-called *quantum simulations* (QSs), which exploit a well-controlled quantum system to study a complicated interacting model [1]. In particular, the QS of *magnetic ordering* is a promising direction of research. Although this effect was already identified by the ancient greeks, it still presents some puzzles that would benefit from a quantum simulator since they cannot be efficiently addressed numerically [2]. Among the most prominent platforms for the QS of magnetism, such as neutral atoms or photons [3], trapped ions [4] have the advantage of near unity fidelity in state preparation, individual readout, and a wide tunability of interactions. Here, we investigate the QS of *frustrated magnetism* with trapped ions, a phenomenon that yields a fundamental challenge with important connections to high-temperature superconductivity and other exotic states of matter, such as spin liquids/glasses [2].

Even if the typical distances between trapped ions make a direct dipole-dipole coupling negligible; the long-range Coulomb interaction yields an indirect mechanism whereby the vibrational phonons, coupled to the spins by lasers, mediate a spin coupling [5]. In the seminal work [6], frustration in a 3-ion chain has been achieved by fine tuning the laser frequencies within the collective vibrational band. However, scaling this scheme to larger ion chains may find a fundamental limit: the vibrational band becomes increasingly dense, and the lasers approach a certain resonance. An alternative scheme would use micro-fabricated surface traps [7], but the current ion-heating problems must be overcome to obtain strong-enough interactions. One may instead rely on large trapping non-linearities [8], yet the requirements remain to be met in experiments. Here, we present a different method amenable of being scaled to larger ion numbers that relies on state-of-the-art ion traps and spin-dependent light forces [9].

Trapped ions crystallize in self-organized Coulomb crystals at low temperatures. By tuning the trapping frequencies [10], a linear string of ions undergoes a structural transition to a *two-leg zig-zag ladder* [Fig. 1(a)]. Whereas the linear configuration has been the usual scenario for the QS of magnetism [4], the capabilities of the zig-zag ladder have remained largely unexplored. In this Letter, we fill in such gap. We show that by exploiting the commensurability of the inter-

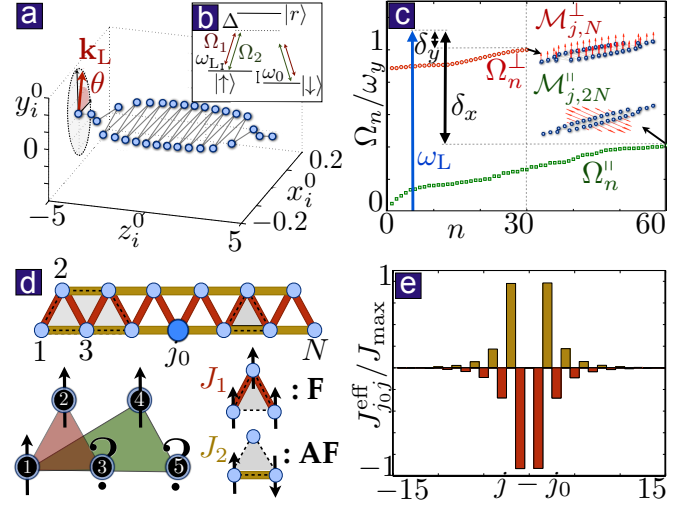


Figure 1. Zig-zag ladder: (a) Equilibrium positions in units of l_z for $N = 30$ ions, $\omega_y \gg \omega_x = 6.1\omega_z$, as given by $\partial(V_{\text{trap}} + V_{\text{Coul}})/\partial r_{j\alpha} = 0$. (b) Scheme of the stimulated Raman transition. A pair of lasers with frequencies ω_1, ω_2 , and wavevectors $\mathbf{k}_1, \mathbf{k}_2$, are far-detuned from the transitions and lead to a two-photon transition $\omega_L = \omega_1 - \omega_2$. (c) Transverse, Ω_n^\perp , and planar, Ω_n^\parallel , normal-mode frequencies. In the inset, the amplitudes of the highest-frequency modes. We also show the frequency ω_L of a laser beam blue-detuned from the vibrational band leading to the transverse spin-dependent force. (d) Scheme of the spin interactions, where $J_1 < 0$ ($J_2 > 0$) is a ferromagnetic (antiferromagnetic) coupling. Incompatible frustration of two plaquettes due to the dipolar range. (e) Coupling between the central ion $j_0 = N/2$ and its neighbors, as obtained for $k_{L,x}l_z = \pi/(x_{j_0}^0 - x_{j_0+1}^0)$.

leg distance of the ladder with the wavelength of the spin-dependent light force, it is possible to control both the relative strength and the sign of the spin interactions in a way that is almost independent of the crystal size, and can be thus scaled to larger ion crystals. We describe how to reach regimes of competing ferromagnetic (F) and antiferromagnetic (AF) couplings, which are incompatible with the crystal geometry so that the groundstate cannot minimize all interactions simultaneously. Therefore, trapped ions can be used as quantum simulators of the two main sources of frustration, namely, *geometric frustration* and *competing interactions*.

Let us summarize our main results: (i) The sign of the spin-

spin interactions between distant ions depends on whether they lie along the same or different rungs of the ladder. (ii) The relative strength of these two interactions can be controlled by tuning the ratio of the inter-leg distance to the wavelength of the light forces. (iii) These ingredients yield a fully-tunable and experimentally-feasible quantum simulator of the J_1 - J_2 quantum Ising model (J_1 - J_2 -QIM), a cornerstone of magnetic frustration [11]. (iv) The long-range character of the spin couplings introduce incompatible sources of frustration leading to a richer phase diagram with a novel conjectured phase.

Model.— We consider N ions of mass m and charge e , confined in a linear trap with frequencies $\{\omega_\alpha\}_{\alpha=x,y,z}$ [12]. The geometry of the Coulomb crystal \mathbf{r}_j^0 , determined by the balance of the trapping forces and the Coulomb repulsion, corresponds to a zig-zag ladder in the x - z plane for $\omega_z < \omega_x \ll \omega_y$ [10]. The vibrations around the equilibrium $\mathbf{r}_j = \mathbf{r}_j^0 + \Delta\mathbf{r}_j$ are coupled through the Coulomb interaction, which yields model of coupled oscillators in the harmonic approximation

$$H = \sum_{j\alpha} \left(\frac{1}{2m} p_{j\alpha}^2 + \frac{1}{2} m \omega_\alpha^2 \Delta r_{j\alpha}^2 \right) + \frac{1}{2} \sum_{jk,\alpha\beta} \gamma_{jk}^{\alpha\beta} \Delta r_{j\alpha} \Delta r_{k\beta}, \quad (1)$$

where $\gamma_{jk}^{\alpha\beta}$ are the vibrational couplings [13]. We identify two types of collective excitations, namely *transverse* and *planar* modes that describe the motion perpendicular and parallel to the crystal in terms of the phonon operators a_n, b_n . The vibration amplitudes $\mathcal{M}_{jn}^\perp, \mathcal{M}_{jn}^\parallel$, and frequencies $\Omega_n^\perp, \Omega_n^\parallel$, are obtained by solving the quadratic problem (1), leading to $H_{\text{ph}} = \sum_{n=1}^N \Omega_n^\perp a_n^\dagger a_n + \sum_{n=1}^{2N} \Omega_n^\parallel b_n^\dagger b_n$ with the phonon branches displayed in Fig. 1(c). As shown in this work, when the planar bandwidth is small enough, a blue-detuned laser beam will only excite the transverse phonons even if it also has a component along the crystal [Fig. 1(a)]. This is a crucial point of our scheme. The transverse phonons, which are best suited to act as carriers of the magnetic interaction, will be responsible of mediating the spin-spin coupling. The component of the laser along the zig-zag plane will not excite the planar phonons, but rather open the possibility of tailoring the ferromagnetic-antiferromagnetic sign of the spin coupling depending on the ratio of the inter-leg ion distance with the wavelength of light.

Effective frustrated spin models.— We consider a pair of laser beams that induce a stimulated Raman transition between two internal states $|\uparrow_j\rangle, |\downarrow_j\rangle$ [Fig. 1(b)]. When the difference between the laser frequencies matches the transverse vibrational frequency, we get a Stark shift $H_d = \frac{\Omega_L}{2} \sum_j \sigma_j^z e^{i\mathbf{k}_L \cdot \mathbf{r}_j^0} e^{i(\mathbf{k}_L \cdot \Delta\mathbf{r}_j - \omega_L t)} + \text{H.c.}$, where σ_j^z is a Pauli matrix, Ω_L is the two-photon Rabi frequency, and \mathbf{k}_L lies in the x - y plane. After introducing the phonons, we make an expansion for small Lamb-Dicke parameters $\eta_{n\perp} = k_{L,y}/\sqrt{2m\Omega_n^\perp} \ll 1$ (similarly for the planar modes). By tuning the laser frequency above the transverse phonon branch, we can neglect all non-resonant terms but the transverse spin-dependent dipole force

$$H_d^\perp = \frac{\Omega_L}{2} \sum_{jn} i e^{i\mathbf{k}_L \cdot \mathbf{r}_j^0} \eta_{n\perp} \mathcal{M}_{jn}^\perp \sigma_j^z a_n^\dagger e^{i\delta_{n\perp} t} + \text{H.c.}, \quad (2)$$

where $\delta_{n\perp} = \Omega_n^\perp - \omega_L$, and we work in a frame rotating with the phonons. For this approximation to hold, the following conditions must be satisfied: $\Omega_L \ll \omega_L$, $\eta_{n\perp} \Omega_L \ll |\Omega_n^\perp - \omega_L|$. The first condition is necessary to suppress the carrier terms, and the second one to avoid the coupling of the spins to the planar modes, and are both satisfied for the realistic parameters below. Additionally, by aligning the lasers nearly parallel to the y -axis, we favor the fulfillment of the last condition.

The conditional force (2), which couples the spins to the transverse phonons, induces a spin interaction due to the virtual exchange of phonons. The exact expression is obtained by a Lang-Firsov-type transformation [14],[5] that decouples spins and phonons $e^{-S}(H_{\text{ph}} + H_d^\perp)e^S \approx H_{\text{eff}} + H_{\text{ph}}$, where $S = \frac{\Omega_L}{2} \sum_{jn} i e^{i\mathbf{k}_L \cdot \mathbf{r}_j^0} \frac{\eta_{n\perp}}{\delta_{n\perp}} \mathcal{M}_{jn}^\perp \sigma_j^z a_n^\dagger - \text{H.c.}$ generates a spin-dependent displacement. This leads to an effective Ising model

$$H_{\text{eff}} = \sum_{j \neq k} J_{jk}^{\text{eff}} \sigma_j^z \sigma_k^z - h \sum_j \sigma_j^x, \quad (3)$$

$$J_{jk}^{\text{eff}} = - \sum_n \frac{\Omega_L^2 k_L^2 \sin^2 \theta}{8m\Omega_n^\perp \delta_{n\perp}} \mathcal{M}_{jn}^\perp \mathcal{M}_{kn}^\perp \cos(\mathbf{k}_L \cdot \mathbf{r}_{jk}^0),$$

where the transverse field, h , follows from a microwave resonant with the transition, and σ_j^x is a Pauli matrix. In this work, we are interested in the anisotropy of $J_{jk}^{\text{eff}} \propto \cos(\mathbf{k}_L \cdot \mathbf{r}_{jk}^0)$, which has been overlooked so far since it vanishes for linear ion chains. Remarkably, it can lead to magnetic frustration in planar crystals. In the limit of tight transverse confinement,

$$J_{jk}^{\text{eff}} = \frac{J_{\text{eff}} \cos \phi_{jk}}{|\mathbf{r}_j^0 - \mathbf{r}_k^0|^3}, \quad J_{\text{eff}} = \frac{\Omega_L^2 \eta_y^2 \omega_z^2}{8\delta_y^2 \omega_y}, \quad \phi_{jk} = k_{L,x} l_z (x_j^0 - x_k^0) \quad (4)$$

where $\eta_\alpha = k_{L,\alpha}/\sqrt{2m\omega_\alpha}$, and $l_z = (e^2/m\omega_z^2)^{1/3}$ gives a unit for the distances. A crucial observation for the QS of frustration is that the sign of the couplings may be different for ions that belong to the same rung of the ladder, or to distinct ones. More precisely, if the condition $k_{L,x} l_z = n\pi/(x_j^0 - x_{j+1}^0)$ is fulfilled for a pair of ions in the bulk of the crystal such that n is an integer, we obtain a ferromagnetic (antiferromagnetic) coupling between pairs of ions in different (same) rungs. We corroborate this claim by obtaining the exact couplings from the numerical solution of Eq. (3), which yields the aforementioned sign alternation [Fig. 1(e)] in agreement with the approximate description (4). Let us highlight the importance of this result: the groundstate shall not be able to minimize such spin-spin couplings simultaneously, and will thus yield a frustrated magnet [Fig. 1(d)]. According to the Toulouse-Villain criterion [15], our spin model (3) is frustrated since there is an *odd* number of **AF** couplings per unit cell. In the following, we support this analytical derivation with numerical simulations on the basis of the realistic experimental settings and parameters that are described now.

Experimental setup.— To realize the spin model (3), we rely on trapped-ion quantum-processing technologies developed to a high degree of perfection [16]. We emphasize that all procedures and experimental parameters are well in reach with current experimental standards. Cold-ion crystals are kept in

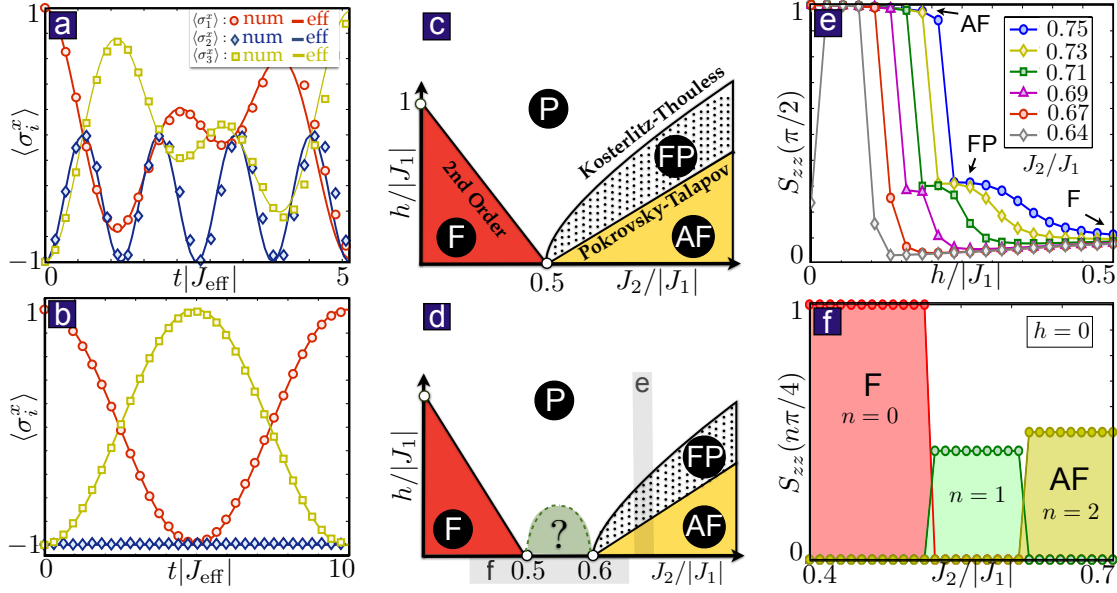


Figure 2. **QS of the frustrated quantum Ising model:** (a) Dynamics of $\langle \sigma_i^x(t) \rangle$ for an initial spin excitation $|+\rangle_1$ in the *allowed-hopping* regime. Comparison of the analytical description H_{eff} , and the numerical study of the complete Hamiltonian $H_{\text{ph}} + H_d$ where the phonon Hilbert space is truncated to one excitation. (b) In the *inhibited-hopping* regime, there is a complete agreement between both descriptions, where the spin excitation cannot occupy site 2. (c) Schematic phase diagram of the J_1 - J_2 -QIM with ferromagnetic (F), dimerized antiferromagnetic (AF), paramagnetic (P), and floating (FP) phases. (d) Conjectured phase diagram with dipolar interactions. Also highlighted in grey the regions studied in (e)-(f). (e) $q = \pi/2$ component of the structure factor evidencing the AF-FP-P transitions. (f) Different magnetic modulations at $h = 0$ showing the splitting of the critical points with a different order in between. (structure-factor components are normalized with respect to the maximum).

linear Paul traps with a combination of static and dynamic electric fields [12]. The specific case in Fig. 1(a) requires a significant anisotropy of the radial confinement ω_x, ω_y , which can be achieved by deforming the symmetric four-rod trap electrode configuration. Additionally, the anisotropy can be increased and tuned to the desired value by applying a bias voltage to the DC electrodes. In this way, the desired zig-zag crystal is trapped with MHz trap frequencies, and fulfilling the condition $\omega_z < \omega_x \ll \omega_y$. The spins in the generic level scheme in Fig. 1(b) might correspond to the hyperfine states of $^9\text{Be}^+$, $^{43}\text{Ca}^+$ ions, or to the Zeeman sub-levels of the ground-state of $^{40}\text{Ca}^+$. These levels are coupled with Raman laser beams that mediate the optical spin-dependent light forces [9].

The experimental sequence consists of a number of steps starting with the (i) initialization of the system. Here, the temperature of all modes is reduced in a Doppler cooling step, followed by a sub-Doppler cooling of the transverse mode. The relatively high frequency $\omega_y/2\pi = 20\text{MHz}$ ensures good cooling results. The spins are initialized by optical pumping, followed by a $\pi/2$ pulse on a resonant Raman transition (not shown in Fig. 1(b)) such that a spin superposition is reached. (ii) The spin-spin interaction is generated by application of the Raman light fields. To suppress spontaneous processes, a large detuning $\Delta > 10\text{GHz}$ is chosen, and light beams with an optical power of about 10mW are focused into a waist of 30 to 60 μm [17] suffice to generate $J_{\text{eff}} \approx 1\text{kHz}$. After an interaction time in the millisecond range, (iii) the simulation result

is readout from the fluorescence imaged on the chip of a CCD camera. For this, we illuminate the entire crystal with light resonant to a dipole-allowed transition such that the $|\uparrow\rangle$ state emits fluorescence while $|\downarrow\rangle$ does not. For the demonstration of frustration, the requirements are much released in comparison to those of full quantum-state tomography [18].

Numerical validation.— We address the simplest scenario where frustration occurs: a 3-ion zig-zag with trap frequencies $\omega_y/\omega_z = 20$, $\omega_x/\omega_z = 1.43$, $\omega_z/2\pi \approx 1\text{MHz}$, leading to $\mathbf{r}_j^0/l_z \in \{(-0.22, 0, -0.92), (0.44, 0, 0), (-0.22, 0, 0.92)\}$. We test the crucial assumption underlying the derivation of the frustrated Hamiltonian (3), namely the possibility to neglect the pushing force on the planar modes. Even if the dipole force only acts in the x - y plane, the z -motion gets coupled through the Coulomb interaction. Hence, we must solve numerically the dynamics of the complete Hamiltonian $H_{\text{ph}} + H_d$, and compare it to the effective analytical description H_{eff} in (3), where we set $h = 0$, $|\psi_0\rangle = |+\rangle_1 \otimes |-\rangle_2 \otimes |-\rangle_3$, with $|\pm\rangle = (|\uparrow\rangle \pm |\downarrow\rangle)/\sqrt{2}$, and consider a ground-state cooled crystal for simplicity. We study two regimes: (i) Allowed hopping: We set $\eta_y = 0.1 = 10\eta_x$, $\omega_L = 1.2\omega_y$, $\Omega_L = 0.1|\omega_y - \omega_L|/\eta_y$, and study the evolution of the whole spin-phonon system for $k_{L,x} = 0$. Since there is no modulation of the coupling sign, the initial spin excitation located at site 1 hops around the triangular plaquette as a consequence of the Ising coupling. In Fig. 2(a), we show the agreement between the analytical and the numerical descriptions. (ii) Inhibited hopping: We use the

same parameters, but set $k_{L,x} = \pi/2l_z(x_2^0 - x_1^0)$. It follows that the Ising couplings between 1-2 and 2-3 vanish $J_{12}^{\text{eff}} = J_{23}^{\text{eff}} = 0$, and thus the excitation only tunnels along $1 \leftrightarrow 3$, as confirmed by both analytical and numerical descriptions in Fig. 2(b).

Due to the complexity of the spin-phonon system, the numerics for ground-state cooled crystals already exhaust the capabilities of classical computers. However, by studying the corresponding Heisenberg equations, one finds $\langle \sigma_j^x(t) \rangle = \langle \sigma_j^x(t) \rangle_{\text{eff}}(1 - \varepsilon)$, where the finite temperature leads to $\varepsilon \propto \sum_n \bar{N}_n^\perp \Omega_{L,n}^2 \eta_{n,\perp}^2 \mathcal{M}_{jn}^\perp \mathcal{M}_{jn}^\perp / \delta_{n,\perp}^2$, with $\bar{N}_n^\perp = \langle a_n^\dagger a_n \rangle_{\text{th}}$. Therefore, there exists a trade-off between strong spin-spin interactions and small residual errors, namely, the larger the laser Rabi frequency is, the stronger the spin interactions become but also the bigger the residual error gets. We have found a compromise for the two, such that for tight confinement and the above parameters, this error is roughly $\varepsilon \approx 10^{-2} \bar{N}$, and thus ground-state cooling is not required. Another possible source of error is the micromotion [12], which may cause heating, or modify the spin-dependent force by additional sidebands. The heating is negligible far from the structural transition where non-linearities are small. Additionally, the effect of the micromotion sidebands can be neglected if $\omega_0 \gg \Omega_{\text{rf}}$, and $\omega_L \approx \omega_y \ll \Omega_{\text{rf}}$, where Ω_{rf} is the r.f. trap frequency.

Frustrated quantum Ising model.— To describe the essence of our quantum simulator, we review the main features of the next-to-nearest neighbor quantum Ising model (J_1 - J_2 -QIM), $H = J_1 \sum_j \sigma_j^z \sigma_{j+1}^z + J_2 \sum_j \sigma_j^z \sigma_{j+2}^z - h \sum_j \sigma_j^x$, in the frustrated regime $\text{sign}(J_2) = -\text{sign}(J_1) = +1$. For both $J_2, h \rightarrow 0$, one finds a ferromagnetic two-fold ground-state $|F\rangle \in \text{span}\{|\uparrow\uparrow\uparrow\cdots\uparrow\uparrow\rangle, |\downarrow\downarrow\downarrow\cdots\downarrow\downarrow\rangle\}$. For $J_1, h \rightarrow 0$, the ground-state is a four-fold dimerized anti-ferromagnet $|AF\rangle \in \text{span}\{|\uparrow\downarrow\uparrow\downarrow\cdots\uparrow\downarrow\rangle, |\downarrow\uparrow\downarrow\uparrow\cdots\downarrow\uparrow\rangle, |\uparrow\uparrow\downarrow\downarrow\cdots\uparrow\uparrow\rangle, |\downarrow\downarrow\uparrow\uparrow\cdots\downarrow\downarrow\rangle\}$. The **F-AF** phase transition is known to be of first order with an exponentially degenerate ground-state at $|J_1| = 2J_2$, which is a hallmark of frustration. Making $h \gg |J_1|, J_2$, the ground-state becomes a paramagnet with the spins aligned with the transverse field $|P\rangle = |\rightarrow \rightarrow \rightarrow \cdots \rightarrow \rightarrow\rangle$. The transitions between the ordered phases mentioned above and the disordered paramagnet yields a rich phase diagram [Fig. 2(c)]. Indeed, both numerical [19] and analytical [20] methods hint at the existence of a new phase separating the **AF-P** transition. This critical phase, commonly denoted as the *floating phase* (**FP**), exhibits quasi-long range order in combination with an incommensurate periodic modulation of the spin-spin correlators that depends on the couplings. We stress that the existence of the **FP** has raised some controversy [21], which makes a QS of the utmost interest to settle the problem.

Our QS naturally includes the effect of longer-range interactions, which may be expected to play an important role in the presence of frustration. Using a Lanczos algorithm optimized for our dipolar model (3), we have diagonalized systems of up to 24 spins, and considered a homogeneous lattice spacing with $\sigma_{N+1}^\alpha = \sigma_1^\alpha$ in order to capture the bulk properties of the ion crystal. To identify the different phases,

we have computed the magnetic structure factor $S_{zz}(q) = \sum_{j,k} \langle \sigma_j^z \sigma_k^z \rangle e^{iq(j-k)}$ with $q \in [0, 2\pi)$, which is an order parameter accessible in trapped-ion experiments (see below). In Fig. 2(d), we summarize our main results, according to which the ordered phases of the next-to-nearest neighbor model survive to the longer-range interactions. This is evidenced in Fig. 2(e), where we show that the $S_{zz}(\pi/2)$ component of the structure factor captures the dimerized-antiferromagnetic and the floating phases. As one crosses the floating phase and enters in the paramagnetic region, the two different types of decay are consistent with the **AF-FP** Pokrovsky-Talapov and the continuous **FP-P** Kosterlitz-Thouless phase transitions.

Remarkably, our results show that the longer dipolar range is crucial in the strongly-frustrated regime $|J_1| \approx 2J_2$. We find that the additional couplings split the **F-AF** critical point, and moreover we conjecture that they give rise to a new phase [Fig. 2(d)]. The different ordering in this central region is a consequence of the competing frustration mechanisms introduced by the long range [Fig. 1(d)]. By including consecutive terms of the dipolar tail, we have checked that the splitting of the critical points is caused by the third- and fourth-nearest neighbors couplings. By increasing these couplings at the expense of the nearest- and next-to-nearest-neighbor interactions, the size of this central region grows. Besides, its robustness is not modified by including further longer-range terms, such as fifth- and sixth-neighbor interactions. In Fig. 2(e), one observes that this new central region supports a different ordering, as evidenced by the existence of a modulation in the structure factor with momentum $q = \pi/4$ not present in the **F**, and **AF** phases. We have checked the decay of this component as one moves into the **P** phase, which supports this conjecture.

Efficient detection methods for the phase diagram.— Since full quantum state tomography becomes inefficient for many-body systems, we focus on the measurement of the order parameters above. One of the advantages of trapped ions with respect to other platforms is their ability to perform high-accuracy measurements at the single-particle level [12]. From the spatially resolved state-dependent fluorescence, one can infer local observables $m_{j,z} = \langle \sigma_j^z \rangle = \frac{1}{2}(P_j^e - 1)$, or two-body correlators $C_{zz}(\mathbf{r}_j^0, \mathbf{r}_k^0) = \langle \sigma_j^z \sigma_k^z \rangle = \frac{1}{4}[1 - 2(P_j^e + P_k^e) + 4P_{j,k}^{e,e}]$. An alternative is to measure global properties of the light emitted by the ion ensemble, which carries information about the spin correlations [22]. The fluorescence spectrum along a detection direction, $\hat{\mathbf{r}}$, is related to the structure factor $\mathcal{S}_{\hat{\mathbf{r}}}(\omega) \propto \sum_{ij} e^{ik\hat{\mathbf{r}} \cdot (\mathbf{r}_i^0 - \mathbf{r}_j^0)} \langle (1 + \sigma_i^z)(1 + \sigma_j^z) \rangle$, where $k = \omega/c$ is the wavevector of the emitted light. Even if the ion spacing is larger than the optical wavelength, one may compensate it by placing the detector orthogonal to the crystal plane, and using a good angular resolution. Note that such structure factors may be used to obtain a lower bound on entanglement [23].

Conclusions and outlook.— We have demonstrated theoretically that cold Coulomb crystals can be used as quantum simulators of paradigmatic, yet controversial, models of frustrated quantum spins. We presented a method to control the **F-AF** nature of an Ising spin-spin interaction between the ions

trapped in a zig-zag structure, leading to a quantum simulator of the J_1 - J_2 quantum Ising model with dipolar range. We have discussed the experimental feasibility of the proposed work and corroborated it by numerics based on experimentally realistic parameters. Analogous ideas can be transferred to different geometries in self-assembled Coulomb crystals, or surface microtraps, to realize other frustrated models. These ideas might also be relevant to atoms confined in multimode optical cavities

Acknowledgements.— This work was supported by the EU STREP projects HIP, PICC, AQUATE, QESSENCE, and by the Alexander von Humboldt Foundation. We thank R. Nigmatullin and D. Porras for useful discussions.

-
- [1] R.P. Feynman, *Int. J. Theo. Phys.* **21**, 467 (1982).
 - [2] S. Sachdev, *Quantum Phase Transitions* (Cambridge University Press, Cambridge, 1999); L. Balents, *Nature* **464**, 199 (2010).
 - [3] J. Simon, et al., *Nature* **472**, 307 (2011); J. Struck, et al., arXiv: 1103.5944 (2011); X.-S Ma, et al., *Nat. Phys.* **7**, 399 (2011).
 - [4] A. Friedenauer, et al., *Nat. Phys.* **4**, 757 (2008); R. Islam, et al., *Nat. Comm.* **2**, 377 (2011).
 - [5] D. Porras, et al., *Phys. Rev. Lett.* **92**, 207901 (2004).
 - [6] K. Kim, et al. *Nature* **465**, 590 (2010).
 - [7] J. Chiaverini, et al., *Phys. Rev. A* **77**, 022324 (2008); J. Labaziewicz et al., *Phys. Rev. Lett.* **100**, 013001 (2008).
 - [8] R. Schmied, et al., *New J. Phys.* **10**, 045017 (2008).
 - [9] C. Monroe, et al., *Science* **272**, 1131 (1996); D. Leibfried, et al., *Nature* **422**, 412 (2003); P. C. Haljan, et al., *Phys. Rev. Lett* **94**, 153602 (2005).
 - [10] J. P. Schiffer, *Phys. Rev. Lett.* **70**, 818 (1993); S. Fishman, et al. *Phys. Rev. B* **77**, 064111 (2008); A. Retzker, et al., *Phys. Rev. Lett.* **101**, 260504 (2008).
 - [11] This system is also known as the axial next-nearest neighbor Ising model (ANNNI), W. Selke, *Phys. Rep.* **170**, 213 (1988).
 - [12] D. J. Wineland, et al., *J. Res. Natl. I. St. Tech.* **103**, 259 (1998); D. Leibfried, et al., *Rev. Mod. Phys.* **75**, 281 (2003).
 - [13] $\gamma_{jk}^{\alpha\beta} = eQ_{jk}^{\alpha\beta}/|\mathbf{r}_{jk}^0|^5 - \delta_{jk} \sum_{l \neq j} eQ_{jl}^{\alpha\beta}/|\mathbf{r}_{lj}^0|^5$, where $\mathbf{r}_{jk}^0 = \mathbf{r}_j^0 - \mathbf{r}_k^0$, $Q_{jk}^{\alpha\beta} = -e[3(\mathbf{r}_{jk}^0)_\alpha(\mathbf{r}_{jk}^0)_\beta - \delta_{\alpha\beta}(\mathbf{r}_{jk}^0)^2]$, and $\hbar = 1$.
 - [14] F. Mintert, et al., *Phys. Rev. Lett.* **87**, 257904 (2001).
 - [15] J. Villain, *J. Phys. C* **10**, 1717 (1977).
 - [16] T. Monz, et al., *Phys. Rev. Lett.* **106**, 130506 (2011).
 - [17] U. G. Poschinger, et al., *Phys. Rev. Lett.* **105**, 263602 (2010).
 - [18] H. Häffner, et al., *Nature* **438**, 643 (2005).
 - [19] M. Beccaria, et al., *Phys. Rev. B* **73**, 052402 (2006); *ibid* **76**, 094410 (2007).
 - [20] D. Allen et al., *J. Phys. A: Math. Gen.* **34**, L305 (2001).
 - [21] T. Shirahata, et al., *Phys. Rev. B* **65**, 024402 (2002); R. Derian, et al., *J. Phys. Soc. Jpn.* **75**, 114001 (2006).
 - [22] R. H. Lehmberg, *Phys. Rev. A* **2**, 883 (1970); I. de Vega, et al., *Phys. Rev. A* **77**, 051804(R) (2008).
 - [23] M. Cramer, et al., *Phys. Rev. Lett.* **106**, 020401 (2011).
 - [24] S. Gopalakrishnan, B. L. Lev, and P. M. Goldbart, arXiv:1108.1400 (2011).